

Mixing Zone Optimization of a Rich-Burn/Quick-Mix/Low-Burn Combustor

M. Blomeyer,* B. Krautkremer,* and D. K. Hennecke†
Darmstadt University of Technology, Darmstadt 64287, Germany
and
T. Doerr‡
BMW Rolls-Royce Aero Engines, Dahlewitz 15827, Germany

The mixing process of hot primary zone gases with secondary air must be rapid and intense for an advanced low NO_x gas turbine based on a rich-burn/quick-mix/lean-burn (RQL) combustor. The injection of multiple jets normal into a confined crossflow is a key technology for this combustion concept. Therefore, an experimental investigation of a nonreacting mixing process of jets in a crossflow was conducted. The jets were injected through one stage of opposed rows of circular orifices into a slightly heated crossflow within a rectangular duct with no annular bypass. All geometries were tested with in-line and staggered arrangements of the centerlines of the opposed jets. Using the analogy of heat and mass transfer the temperature distribution was measured, and from that the mixing rate was determined for parametric variation of flow and geometric conditions. In accordance with the application to RQL combustion, emphasis was put on high momentum-flux ratios with high mass flow addition. The mixing process was found to be minimally affected by mainstream Reynolds number and mainstream turbulence, but significantly influenced by the addition of swirl to the mainstream. Correlations based on the experimental data were developed describing best mixing depending as a function of geometric conditions (duct height to hole diameter ratio, relative spacing of adjacent jets) and jet to crossflow momentum-flux ratio.

Nomenclature

A	= area
c_D	= discharge coefficient
d	= jet diameter
d_{sw}	= diameter of the swirler exit
h	= height of the mixing zone
J	= momentum-flux ratio, $\rho_j v_j^2 / \rho_\infty v_\infty^2$
Le	= Lewis number, Pr/Sc
\dot{m}	= mass flow
n	= number of data points in y - z planes
Pr	= Prandtl number
p	= static pressure
Re	= Reynolds number
Sc	= Schmidt number
S_N	= swirl number
s	= spacing between adjacent jets
T	= temperature
T_{adb}	= equilibrium temperature
v	= velocity
w	= width of the duct
x	= downstream location from jet centerline
y	= lateral distance from middle of channel
z	= vertical distance from middle of channel
γ	= concentration distribution, dimensionless
θ_{adb}	= equilibrium temperature, dimensionless
ρ	= density
σ	= standard deviation from mean temperature

Subscripts

eff	= effective
i	= local value
j	= jet
m	= mean value
max	= maximum
norm	= normalized by relating to the maximum
∞	= mainstream

Introduction

THE knowledge about the effects of aircraft engine exhaust at high altitudes along with increasing public awareness of environmental issues has led to the stringent regulation of pollutant emissions.¹ In contrast to unburnt hydrocarbons (UHC) and carbon monoxides (CO), which have been significantly reduced, there has been no diminution in oxides of nitrogen (NO_x) emission. To meet the future NO_x reduction requirements, the development of low-emission combustors was intensified. In addition to the lean combustion and the lean premixed prevaporized combustion, the concept of rich-burn/quick-mix/lean-burn (RQL) combustion is a promising approach to reduce NO_x emissions.² The NO_x formation is diminished, avoiding stoichiometric combustion by dividing the combustion chamber into two stages. The primary stage is operated under fuel-rich conditions. In the following mixing section, air is added to achieve lean conditions in the second stage. The success of this concept relies on the rapid and homogeneous mixing to minimize residence time and zones under stoichiometric conditions.³

The lack of suitable tools for the mixing zone design was the reason for an experimental study of a nonreacting mixing process of jets with a crossflow. To determine the degree of mixedness of two gaseous streams, the concentration distribution must be measured in a plane perpendicular to the flow direction. However, the analysis of gaseous samples takes a very long time. This disadvantage was avoided using the analogy of heat and mass transfer. The mainstream was slightly heated up (thermal indication), and temperature distribution

Received Sept. 25, 1997; revision received July 13, 1998; accepted for publication July 27, 1998. Copyright © 1998 by the American Institute of Aeronautics and Astronautics, Inc. All rights reserved.

*Research Assistant, Department of Gas Turbines and Flight Propulsion, Petersenstr. 30.

†Professor, Department of Gas Turbines and Flight Propulsion, Petersenstr. 30.

‡Combustion Scientist, Combustor Department, Eschenweg 11.

was measured downstream of the jet injection for the determination of mixedness.

Previous investigations^{4,5} of crossflow mixing have concentrated on temperature profile development in dilution zones of combustors characterized by low momentum-flux ratios along with low mass flow addition. Recent studies have presented the mixing process of jets injected perpendicularly into a crossflow in cylindrical⁶⁻⁹ and rectangular¹⁰⁻¹³ ducts. The effects of the inlet flow conditions were discussed in latest publications.^{14,15}

The first part of this paper shows the admissibility of the analogy of heat and mass transfer. In the following part, the effects of varying inlet flow conditions of the mainstream on mixing is discussed. The main part presents the correlations for optimum mixing derived from the experimental results. The effect of mainstream swirl on the mixing process is described in the final part of this paper. To get a comprehensive view of this topic, a wide range of geometric and flow parameters was chosen. There is particular emphasis on high momentum-flux ratios combined with high mass-flow ratios of jet to mainstream to meet the requirements of the RQL combustion.

Experiments

Figure 1 is a schematic representation of the atmospheric mixing chamber. It consists of three parallel ducts of constant rectangular cross sections. The inner duct is 300 mm in width and 100 mm in height. The outer flow channels are of the same width and 60 mm in height. The upper and lower jet streams and the mainstream pass settling chambers, flow straighteners with nozzles and enter the mixing section. Two exchangeable flat plates of 2 mm thickness separate the inner channel from the outer ones. The jet streams were injected through a single stage of opposed rows of circular sharp-edged orifices that were machined into these plates.

The mass flow of each stream is determined by orifice flow meters. Conventional pressure transducers in combination with scanivalve devices provide the pressure acquisition. At the inlet, the mainstream temperature is $T_\infty \approx 325$ K and the flow velocity is $v_\infty = 10$ m/s, with a turbulence level of approximately 1%. The jet stream enters the mixing chamber with a temperature $T_j \approx 300$ K. The temperature distribution is measured by traversing a probe in the y - z planes up to $x/h = 1$ downstream of the injection port. An iron-constantan thermocouple is used with a bent design (90 deg) to reduce the impact on the flowfield. The relative error as a result of that temperature measurement technique is about 3%. For the validation of the heat and mass transfer analogy, carbon dioxide (CO_2) was injected into the mainstream far upstream of the jet-injection plane. Gas samples were sucked off by a tubing pump through a pitot probe that was also traversed in y - z planes. The samples were analyzed by an NDIR-analyzer (non-dispersive infrared analyzer). The three-axis traversing mechanism, the data acquisition, and the operation of the test rig is controlled by a personal computer.

The momentum-flux ratio J and the geometric conditions of the jet injection (s/d , h/d) have been parametrically varied, keeping the mainstream conditions constant. In contrast to real combustors, the density ratio ($\rho_j/\rho_\infty = T_\infty/T_j$) was about 1.1 (real gas turbine ~ 3). Keeping the momentum-flux ratio con-

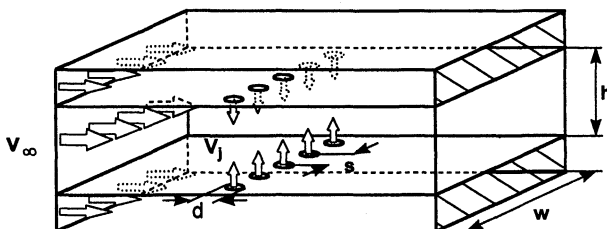


Fig. 1 Schematic of multiple jet mixing.

Table 1 In-line mixing configurations

s/d	h/d				
	5	6.67	10	12.5	20
1.5	x	—	x	x	x
2	x	x	x	x	x
3	x	—	x	x	—
4	—	—	x	x	x
6	x	—	x	x	x

Table 2 Staggered mixing configurations

s/d	h/d					
	2.5	3.3	5	6.67	10	12.5
1.5	x	—	—	—	—	—
1.75	—	x	—	—	—	—
2	—	—	x	—	—	—
2.25	—	—	—	x	—	—
3	—	—	x	x	x	—
3.5	—	—	—	—	—	x
4	—	—	x	x	x	x
6	—	—	x	x	x	x

stant, the influence of the density ratio on the mixing process and on jet penetration is of second order.⁵

Mixing Configurations

Tables 1 and 2 show the configurations investigated. Jet to mainstream J was varied within the range of 5 and 300 to obtain optimum mixing for each configuration.

The corresponding mass-flow ratio can be determined using the following equation:

$$\frac{2}{\pi \times c_D} \times \frac{s}{d} \times \frac{h}{d} = \sqrt{\frac{\rho_j}{\rho_\infty}} \times \sqrt{J} \times \left(\frac{m_j}{\dot{m}_\infty}\right)^{-1} \quad (1)$$

Turbulence and Swirl-Generating Devices

Within the scope of the foregoing studies, an active turbulence generator was placed in the mainstream $5h$ upstream of the injection plane. The mainstream turbulence level was determined by means of hot-wire anemometry. It could be raised from 3% up to 10%. A detailed description of the turbulence generator is given by Doerr.¹⁶

The effect of burner-induced swirl on the mixing process was investigated by using a three-swirler bulkhead placed $0.75h$ upstream of the injection plane. The movable block swirl generators^{17,18} allow the mainstream swirl number to vary continuously from 0 to 1.

Definition of Mixing Quality

Because of the analogy between heat and mass transfer, temperature is used as an indicator of mixing. Therefore, the degree of mixing can be determined by measuring the distribution of the time-averaged temperature in y - z planes (46×46 points) downstream of the injection ports. The local dimensionless temperature θ_i is defined by

$$\theta_i = (T_i - T_j)/(T_\infty - T_j) \quad (2)$$

$\theta_i = 0$ corresponds to pure jet stream, and $\theta_i = 1$ indicates the mainstream (note that θ also appears in previous studies⁶ determined by $\theta_6 = 1 - \theta_{\text{Blomeyer}}$). Uniform mixing is described by the adiabatic mixing temperature following the conservation equation for energy:

$$T_{\text{adb}} = \frac{\dot{m}_j T_j + \dot{m}_\infty T_\infty}{\dot{m}_j + \dot{m}_\infty} \quad (3)$$

or dimensionless:

$$\theta_{adb} = \sum_{i=1}^n \frac{\dot{m}_i}{\dot{m}_j + \dot{m}_\infty} \times \theta_i = \frac{\dot{m}_\infty}{\dot{m}_j + \dot{m}_\infty} \quad (4)$$

The standard deviation from equilibrium temperature within a y - z plane is calculated as:

$$\sigma_{adb} = \sqrt{\sum_{i=1}^n \frac{\dot{m}_i}{\dot{m}_j + \dot{m}_\infty} \times (\theta_i - \theta_{adb})^2} \quad (5)$$

The maximum standard deviation is presented by a fully separated temperature distribution, which consists only of jet and mainstream temperature. The frequency is given by the partial to total mass-flow ratio, respectively,

$$\sigma_{max,adb} = \sqrt{\theta_{adb} \times (1 - \theta_{adb})} \quad (6)$$

To compare different configurations along with different mass-flow ratios, it is necessary to relate the standard deviation to the maximum one. This normalized deviation is forced, being in the range of zero and unity:

$$\sigma_{norm,adb} = \sigma_{adb} / \sigma_{max,adb} \quad (7)$$

It is sufficient to consider the standard deviation from the mean temperature of a constant y - z plane, far from the injection plane ($x/h \geq 0.5$):

$$\theta_m = \frac{1}{n} \sum_{i=1}^n \theta_i \quad (8)$$

$$\sigma = \sqrt{\frac{1}{n} \sum_{i=1}^n (\theta_i - \theta_m)^2} \quad (9)$$

Significant differences between the standard deviation from equilibrium and the mean temperature can only be observed near the injection plane. But best mixing was found for the same configuration. Subsequently, a determination of the flow-field for mass weighting was terminated. The degree of mixing was expressed by the simplified normalized standard deviation:

$$\sigma_{max} = \sqrt{\theta_m \times (1 - \theta_m)} \quad (10)$$

$$\sigma_{norm} = \sigma / \sigma_{max} \quad (11)$$

This parameter is similar to the square root of the unmixedness parameter used by Refs. 10–14.

Results and Discussion

The first step within the investigation was to verify the validity of the analogy of heat and mass transfer and to check the influence of a variation of mainstream flow conditions, i.e., turbulence level and Reynolds number.

Analogy of Heat and Mass Transfer

For constant-property fluids, the dimensionless conservation laws of energy and species are analogous. Thus, the dimensionless temperature distribution Θ_i is identical to the dimensionless concentration distribution γ_i for a given Reynolds number, if the following condition is fulfilled:

$$Le = 1, \quad \text{i.e., } Pr = Sc \quad (12)$$

For turbulent flowfields, the Lewis number can be sufficiently supposed as unity. Figure 2 shows the distributions for temperature in Fig. 2a, and the concentration in Fig. 2b for the same geometric and flow condition. The excellent agreement

is expressed in the normalized standard deviation, respectively. The difference is less than 1.5%, thus below the accuracy of the measurement technique.

Mainstream Turbulence

The real flowfield of gas-turbine combustors is characterized by high turbulence levels. Within the scope of basic studies, the mainstream turbulence level was continuously increased up to 10% by means of an active turbulence generator. However, no influence on the mixing process was observed (Fig. 3). The mixing process is dominated by the high turbulence that is produced in the shear layer of the jets.

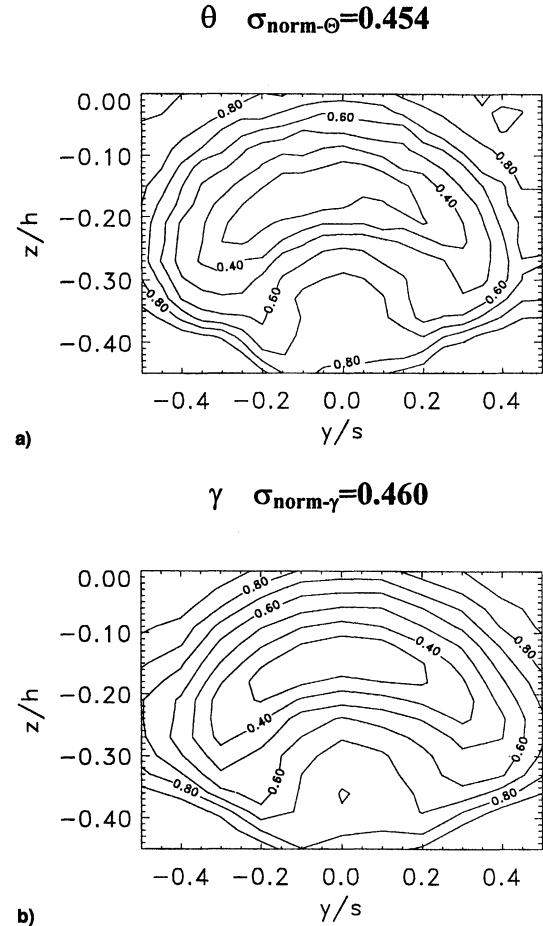


Fig. 2 a) Distributions of temperature and b) concentration, $h/d = 5$, $s/d = 2$, (lower duct half).

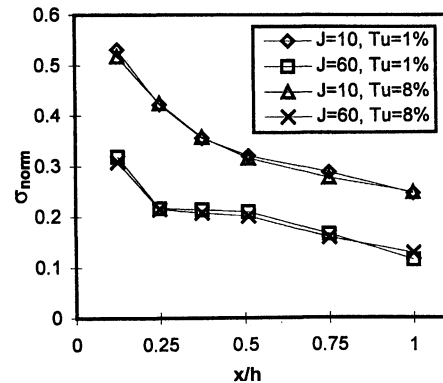


Fig. 3 Influence of mainstream turbulence, $h/d = 10$, $s/d = 2$ in-line.

Mainstream Reynolds Number

Figure 4 shows the influence of Reynolds number variation on the mixing process. The momentum-flux ratio was kept constant for a configuration of $h/d = 10$, $s/d = 2$, and an in-line arrangement. As long as compressibility effects can be neglected (low Mach numbers), no significant influence of mainstream Reynolds number on the standard deviation was observed within the range $25,000 < Re < 55,000$.

In-Line Jet Axis Configuration

For all configurations shown in Table 1, the momentum-flux ratio was increased as far as a minimum standard deviation was reached. It was checked to see that no backflow occurred because it has to be avoided as a result of the application of RQL combustion. Best mixing was found if the opposed jets penetrate into the middle of the channel without impinging on each other (Fig. 5, middle column). For lower momentum-flux ratios, the mainstream remains in the inner part of the channel (Fig. 5, left), higher momentum-flux ratios led to an impinge-

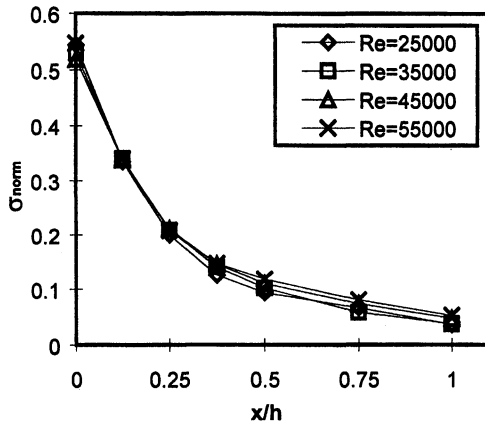


Fig. 4 Influence of mainstream Reynolds number on mixing, $h/d = 10$, $s/d = 2$ in-line.

ment of the jet in the middle (Fig. 5, right). In the latter case, the jet stream remains in the middle. Both led to a separation of jet and mainstream and the mixing quality worsened.

The penetration depth increases with increasing duct height to diameter ratio and relative spacing for constant momentum-flux ratio. For relatively wide spacing, the jets tend to flow back into the primary zone if they impinge on each other in the middle of the duct.

Figure 6 illustrates the relation between the configurations investigated and the momentum-flux ratio for optimum mixing. From this experimental database the following correlation was developed:

$$J_{\text{opt}} = 0.045 \times \left(\frac{h}{d}\right)^2 + \frac{3.08 \times (h/d)^{1.65}}{[(s/d) + 0.26]^{1.29}} \quad (13)$$

The curves in Fig. 6 show the suitability of this correlation. It simplifies the correlation that was developed in Refs. 16 and 19, which contains a slight dependence of downstream position x/h on the momentum-flux ratio for best mixing. The neglect of mass weighting does not permit an accurate determination of mixedness near jet injection. Therefore, the downstream position $x/h = 0.5$ was chosen for the determination of mixing.

Staggered Jet Axis Configuration

The impingement of jets in the middle might be avoided using a staggered jet axis configuration. Relative spacing must be wide enough to compensate the spread of the jets. The following relation was found describing the relative spacing needed in dependence of duct height to diameter ratio^{16,20}:

$$(s/d) \geq 0.2 \times (h/d) + 1 \quad (14)$$

If this condition is fulfilled, the jets pass each other in the middle of the mixing zone as long as the momentum-flux ratio is high enough. According to Eq. (14), the configurations shown in Table 2 were chosen to be investigated. The mixing process was found to be similar to that of the in-line arrange-

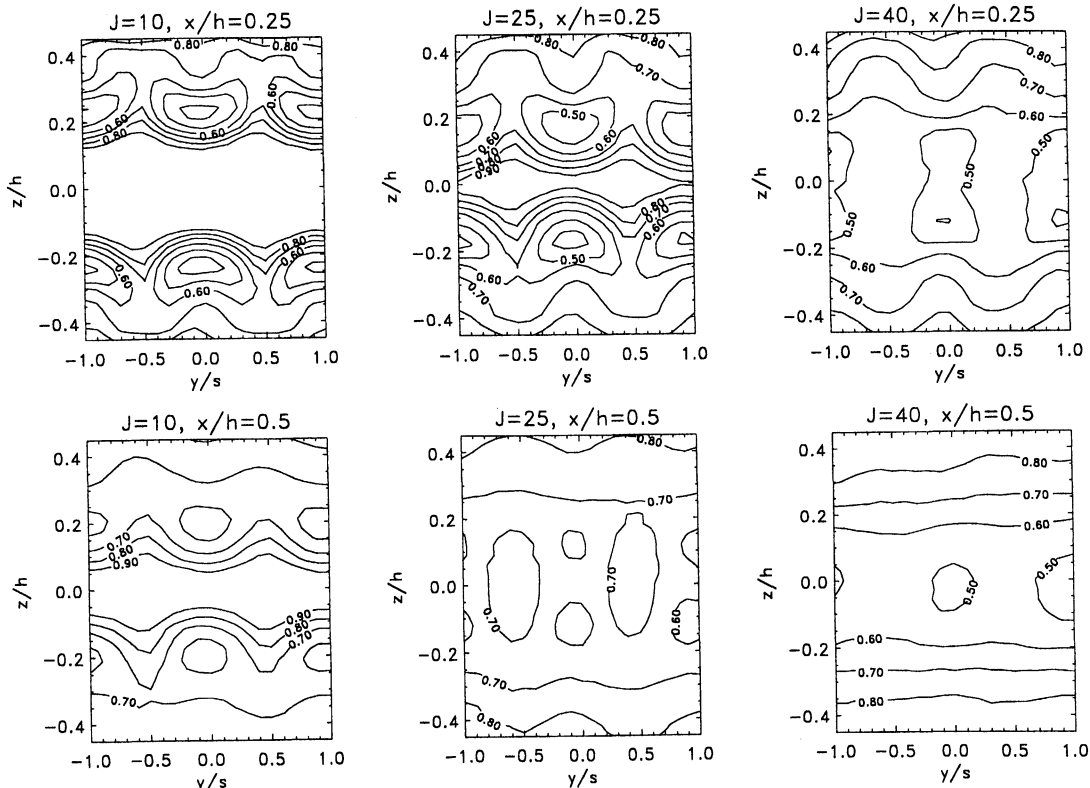


Fig. 5 Temperature distribution, $h/d = 6.67$, $s/d = 2$.

ment of the jets if the penetration depth is less than half the duct height (Fig. 7, left side). For very close spacing, the jets become stuck in the middle if the momentum-flux ratio is not high enough (Fig. 7, middle). The cold jet stream builds a stable stratification that can be observed far downstream. With increasing momentum-flux ratio, only the cores of the jets are pushed through the middle and penetrate into the opposite duct half (Fig. 7, right). The strong shear layers improve the mixing process. The mixing rate remains on that high level even if momentum-flux ratio is raised further. Figure 8 shows the database and the correlation for best mixing:

$$J_{\text{opt}} = 25 \times (h/d)^{0.6} \times \{1 + 0.6 \times [(s/d) - 0.23 \times (h/d)]^{-1.6}\} \quad (15)$$

Effect of Mainstream Swirl

By the addition of swirl to the mainstream, the flow condition is converted into a strong three-dimensional flowfield. Therefore, the convective heat and mass transfer is improved and mixing quality is enhanced. An additional lateral velocity is induced that shifts the jets into the lateral direction (Fig. 9). The penetration depth of the jets is significantly reduced in

comparison without swirl. As a result, best mixing was found for higher momentum-flux ratios (Fig. 10). The additional lateral velocity lowers the effective relative spacing and effective momentum-flux ratio (see Fig. 11). The flow angle and, subsequently, the effective spacing and momentum-flux ratio, can be estimated by the swirl number:

$$\tan \alpha \approx \frac{1}{3} S_N \times (h/d_{\text{sw}}) \times (T_j/T_\infty) \quad (16)$$

$$s_{\text{eff}} = s \times \cos \alpha \quad (17)$$

$$J_{\text{eff}} = J \times \cos^2 \alpha \quad (18)$$

$$S_N = \frac{2 \int_0^{d_{\text{sw}}/2} \rho v_x v_y r^2 dr}{d_{\text{sw}} \int_0^{d_{\text{sw}}/2} (\rho v_x^2 + p) r dr} \quad (19)$$

A relative spacing of $s/d = 2$ is reduced by a swirl number of $S_N = 0.9$ to $s_{\text{eff}}/d \approx 1.7$ ($h/d_{\text{sw}} = 2.5$). The required effective momentum-flux ratio for a duct height to diameter ratio of $h/d = 10$ is calculated with Eq. (13) as $J_{\text{eff}} \approx 65$. The optimum momentum-flux ratio must be $J = J_{\text{eff}}/0.75 \approx 85$ for this swirl number.

Figure 10 illustrates the normalized standard deviation vs downstream position x/h with and without mainstream swirl. The minimum was found for $J = 40$ – 50 in the case without swirl, and for $J = 80$ – 90 with mainstream swirl. In accordance with Eq. (1), the mass flow addition is increased.

This example proves that mainstream swirl is an important parameter and must be taken into account for the mixing zone design.

Comparison to Previous Studies

Extensive research has been performed for the dilution zone mixing process for a single-sided injection.⁶ Optimum rela-

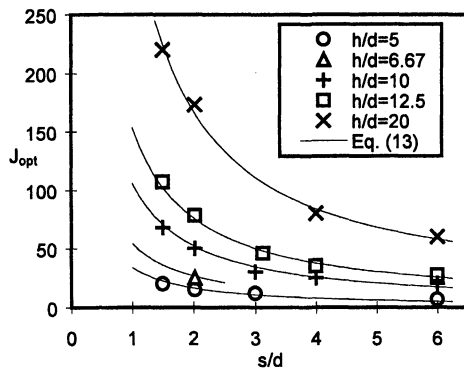


Fig. 6 Best mixing configurations, in-line.

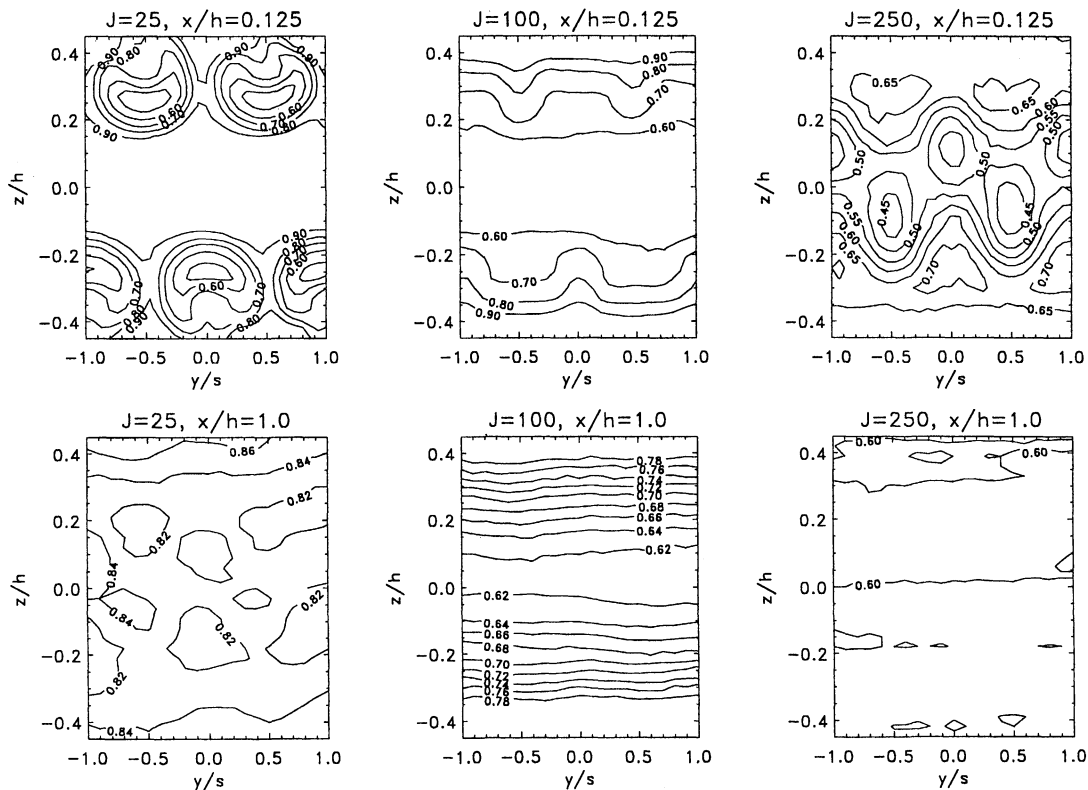


Fig. 7 Temperature distribution, $h/d = 10$, $s/d = 3$.

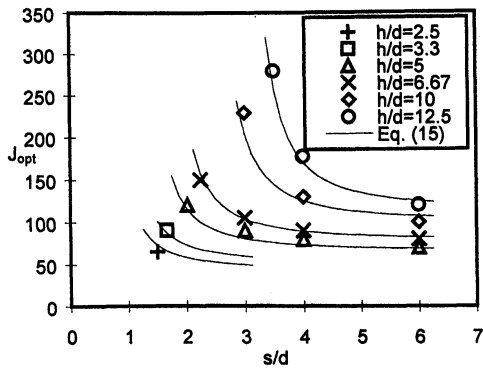
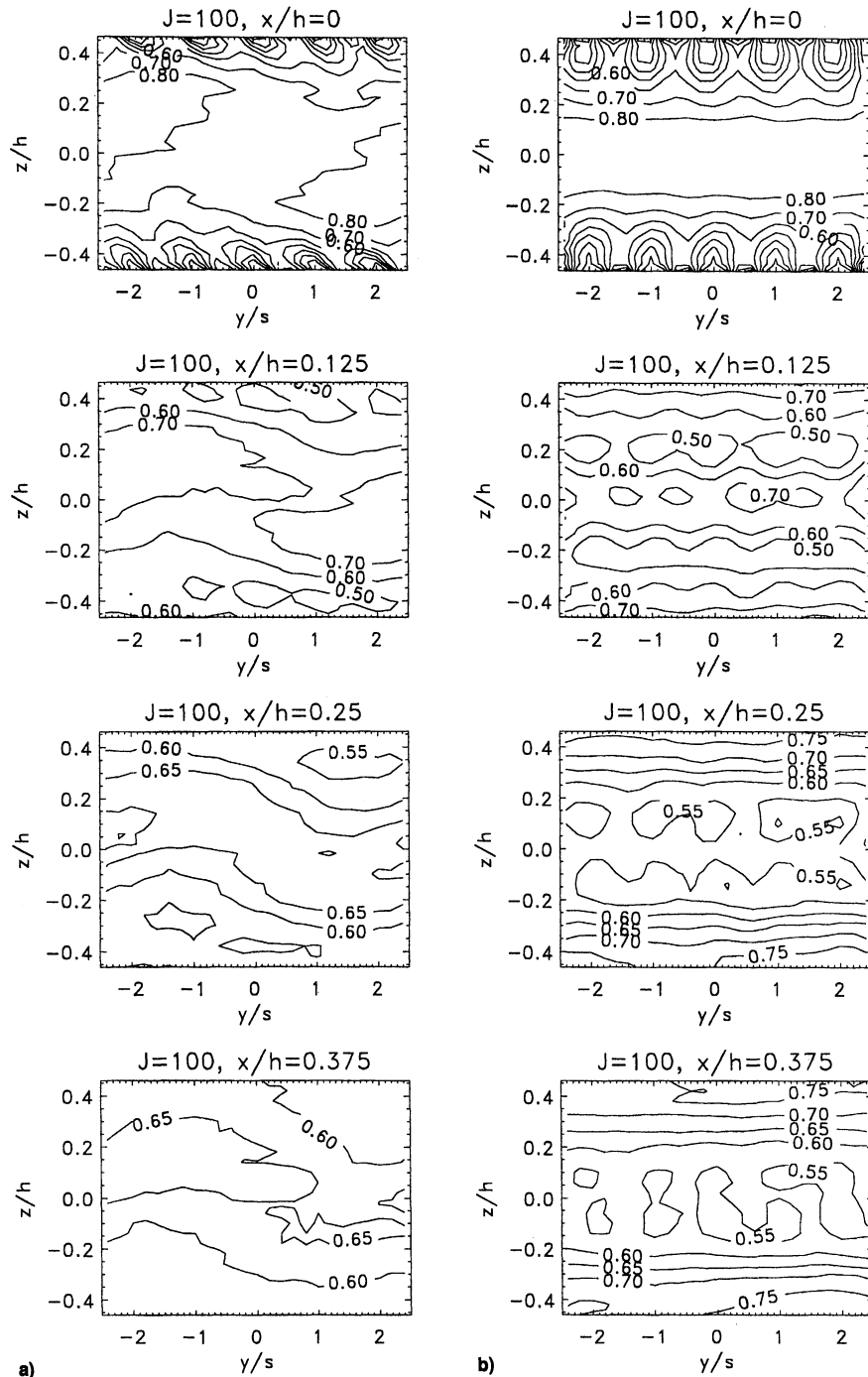


Fig. 8 Best mixing configurations, staggered.

tionships were determined to be a function of $(s/h)(J)^{0.5}$ for the range of conditions tested and analyzed:

$$(s/h)\sqrt{J} = C \quad (20)$$

Optimum mixing was obtained when C was about 2.5. A two-sided injection was studied to a lesser extent. This arrangement was supposed to be similar to one-sided injection if the duct was considered to be sliced in half. Thus, a C of 1.25 would be expected for optimum mixing of opposed rows of jets with centerlines in-line. Very little data were generated for a staggered arrangement. It was suggested that staggered holes produce optimum mixing if the jets penetrate past each other.⁶ It was supposed that best mixing was obtained when alternate jets for optimum one-sided injection were moved to

Fig. 9 Temperature distribution, a) with and b) without mainstream swirl, $h/d = 10$, $s/d = 2$.

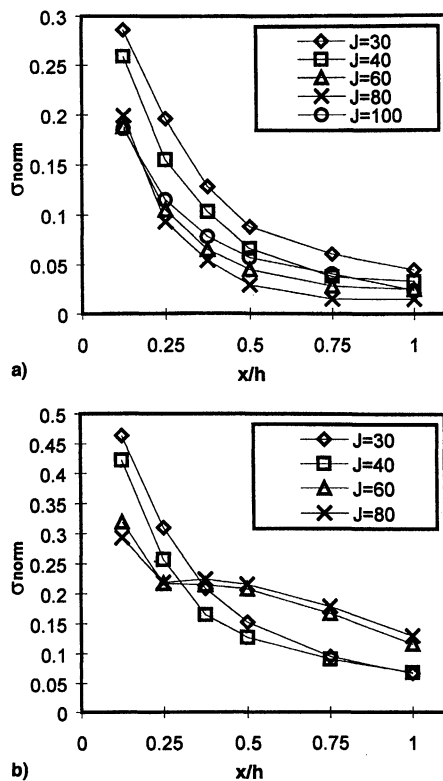


Fig. 10 Standard deviation a) $s/d = 2$, $h/d = 10$, $S_N = 1$ and b) without swirl.

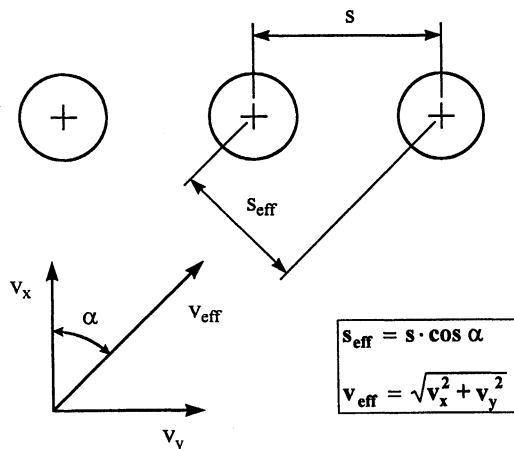


Fig. 11 Influence of mainstream swirl on flow direction.

the opposite wall. Therefore, the correlation constant would be expected to be 5.0 for opposed rows of jets with staggered centerlines.

These correlations are based on experiments for the dilution zone design. Accordingly, a low mass flow ratio (less than 0.5 for a conventional dilution zone vs more than 2.0 for RQL) along with low momentum-flux ratio were investigated. It was shown that these results are not directly applicable because of RQL conditions.^{10,21} It was recommended to change C from 1.25 to 2.5 for an in-line arrangement of the opposed rows.¹⁰ For staggered configurations, C varies from 4 to 6.8 in dependence of the momentum-flux ratio ($16 < J < 64$).²¹

All investigations were concentrated on momentum-flux ratios $J \ll 100$. The implementation of air-blast atomizers for modern combustion chambers results in significantly higher momentum-flux ratios. The validity of Eq. (20) has never been proven for those conditions. The influence of the hole diameter is not negligible, particularly for a staggered jet axis arrange-

ment with close relative spacing. Therefore, advanced correlations such as Eqs. (13–15) are necessary for the mixing zone design of RQL combustors.

Conclusions

The results of investigating a nonreacting mixing process of jets with a confined crossflow can be summarized as follows:

- 1) The analogy of heat and mass transfer can be applied for the determination of the mixing state.
- 2) Mass flow weighting of temperature is not necessary to find optimum flow and geometric conditions for the mixing zone.
- 3) The mixing process is unaffected by mainstream turbulence and mainstream Reynolds number within the range investigated.
- 4) Jet penetration depth increases with increasing duct height to diameter ratio and increasing relative spacing.
- 5) Best mixing is reached for in-line configurations if penetration depth is just below half the mixing zone height.
- 6) For staggered jet axis arrangements, the relative spacing must be wide enough so that the jets pass each other in the middle of the duct and penetrate into the opposite duct half.
- 7) Best mixing configurations for in-line and staggered arrangements are described by Eqs. (13) and (15).
- 8) The presence of swirl reduces effective relative spacing and momentum-flux ratio. Therefore, penetration depth decreases.
- 9) Mainstream swirl must be taken into account for the design of the mixing zone of an RQL combustor.

Acknowledgments

The project presented in this paper was initially supported by the Deutsche Forschungsgemeinschaft. Since 1994, the German Ministry of Research and Technology (task number: 20T9403A) continues, together with BMW Rolls-Royce, to support the investigations within the National Aeronautics Research Program, Engine 3E.

References

- ¹Archer, L., "Aircraft Emissions and the Environment: CO_x SO_x HO_x & NO_x," *OIES Papers*, Parchment Press, Oxford, England, UK, 1993.
- ²Grieb, H., and Simon, B., "Pollutant Emissions of Existing and Future Engines for Commercial Aircraft," *Lecture Notes in Engineering, Air Traffic and the Environment—Background, Tendencies and Potential Global Atmospheric Effects*, Springer-Verlag, Berlin, 1990, pp. 43–83.
- ³Rizk, N. K., and Mongia, H. C., "Low NO_x Rich-Lean Combustion Concept Application," AIAA Paper 91-1962, June 1991.
- ⁴Kamotani, Y., and Greber, I., "Experiments on Confined Turbulent Jets in Crossflow," NASA CR-2392, March 1974.
- ⁵Holdeman, J. D., and Walker, R. E., "Mixing of a Row of Jets with a Confined Crossflow," *AIAA Journal*, Vol. 15, No. 2, 1977, pp. 243–249.
- ⁶Holdeman, J. D., "Mixing of Multiple Jets with a Subsonic Crossflow," *Progress in Energy and Combustion Sciences*, Vol. 19, No. 1, 1993, pp. 31–70; also AIAA Paper 91-2458, June 1991 and NASA TM 104412, 1990.
- ⁷Kroll, J. T., Sowa, W. A., Samuelsen, G. S., and Holdeman, J. D., "Optimization of Circular Orifice Jets Mixing into a Heated Cross Flow in a Cylindrical Duct," AIAA Paper 93-0249, Jan. 1993.
- ⁸Hatch, M. S., Sowa, W. A., Samuelsen, G. S., and Holdeman, J. D., "Jet Mixing into a Heated Cross Flow in a Cylindrical Duct: Influence of Geometry and Flow Variations," AIAA Paper 92-0773, Jan. 1992.
- ⁹Holdeman, J. D., Liscinsky, D. S., Oechsle, V. L., Samuelsen, G. S., and Smith, C. E., "Mixing of Multiple Jets with a Confined Subsonic Crossflow: Part I—Cylindrical Ducts," *American Society of Mechanical Engineers, Paper 96-GT-482*, June 1996; also NASA TM 107185, April 1996.
- ¹⁰Liscinsky, D. S., True, B., and Holdeman, J. D., "Experimental Investigation of Cross Flow Jet Mixing in a Rectangular Duct," AIAA Paper 93-2037, June 1993.
- ¹¹Liscinsky, D. S., True, B., Vranos, A., and Holdeman, J. D., "Ex-

perimental Study of Cross-Stream Mixing in a Rectangular Duct," AIAA Paper 92-3090, July 1992.

¹²Liscinsky, D. S., True, B., and Holdeman, J. D., "Mixing Characteristics of Directly Opposed Rows of Jets Injected Normal to a Crossflow in a Rectangular Duct," AIAA Paper 94-0217, Jan. 1994.

¹³Holdeman, J. D., Liscinsky, D. S., and Bain, D. B., "Mixing of Multiple Jets with a Confined Subsonic Crossflow: Part II—Opposed Rows of Orifices in Rectangular Ducts," American Society of Mechanical Engineers, Paper 97-GT-439, June 1997; also NASA TM 107461, May 1997.

¹⁴Liscinsky, D. S., True, B., and Holdeman, J. D., "Effects of Inlet Conditions on Crossflow Jet Mixing," AIAA Paper 96-2881, July 1996.

¹⁵Blomeyer, M., Krautkremer, B., and Hennecke, D. K., "Optimum Mixing for a Two-Sided Injection from Opposing Rows of Staggered Jets into a Confined Crossflow," American Society of Mechanical Engineers, Paper 96-GT-453, June 1996.

¹⁶Doerr, T., "Ein Beitrag zur Reduzierung des Stickoxydausstoßes von Gasturbinenbrennkammern—Die Optimierung des Mischung-

sprozesses der Fett-Mager-Stufenverbrennung," Ph.D. Dissertation, Darmstadt, Germany, 1995.

¹⁷Leuckel, W., "Swirl Intensities, Swirl Types and Energy Losses of Different Swirl Generating Devices," International Flame Research Foundation, Dok. G 02/a/16, Ijmuiden, The Netherlands, 1967.

¹⁸Mundus, B., "Über den Einfluß der Drallerzeugerkonstruktion auf das Strömungs- und Reaktionsfeld turbulenter Diffusionsflammen," Ph.D. Dissertation, Bochum, Germany, 1990.

¹⁹Doerr, T., Blomeyer, M., and Hennecke, D. K., "Optimization of Multiple Jets Mixing with a Confined Crossflow," American Society of Mechanical Engineers, Paper 95-GT-313, 1995.

²⁰Doerr, T., Blomeyer, M., and Hennecke, D. K., "Experimental Investigation of Optimum Jet Mixing Configuration for RQL-Combustion," International Society of Air Breathing Engines, 95-7044, Sept. 1995.

²¹Bain, D. B., Smith, C. E., and Holdeman, J. D., "Mixing Analysis of Axially Opposed Rows of Jets Injected into Confined Crossflow," *Journal of Propulsion and Power*, Vol. 11, No. 5, 1995, pp. 885–893.

JOURNEY TO THE MOON

*The History of the
Apollo Guidance Computer*

ELDON C. HALL



1996, 226 pp, illus,
Softcover
ISBN 1-56347-185-X
AIAA Members \$29.95
List Price \$54.95



American Institute of Aeronautics and Astronautics
Publications Customer Service, 9 Jay Gould Ct., P.O. Box 753, Waldorf, MD 20604
Fax 301/843-0159 Phone 800/682-2422 8 a.m. – 5 p.m. Eastern

The first of its kind, *Journey to the Moon* details the history and design of the computer that enabled U.S. astronauts to land on the moon. Describing the evolution of the Apollo guidance computer, Mr. Hall contends that the development of the Apollo computer supported and motivated the semiconductor industry just as integrated circuits were emerging—just before the electronics revolution that gave birth to modern computers.

The book recalls the history of computer technology, both hardware and software, and the application of digital computing to missile guidance systems and manned spacecraft.

Contents:

History • Computer Hardware • Computers • MIT Instrumentation Laboratory • Apollo Hardware • Requirements • In the Beginning—Apollo Computer • Winds of Change Were Blowing • Block I Computers • System Integration • Naysayers and Advice from Outside Experts • Next Generation—Block II • Naysayers Revisited • Reliability Apollo Software • Software Development • Mission Software • Finale

CA and VA residents add applicable sales tax. For shipping and handling add \$4.75 for 1–4 books (call for rates for higher quantities). All individual orders, including U.S., Canadian, and foreign, must be prepaid by personal or company check, traveler's check, international money order, or credit card (VISA, MasterCard, American Express, or Diners Club). All checks must be made payable to AIAA in U.S. dollars, drawn on a U.S. bank. Orders from libraries, corporations, government agencies, and university and college bookstores must be accompanied by an authorized purchase order. All other bookstore orders must be prepaid. Please allow 4 weeks for delivery. Prices are subject to change without notice. Returns in salable condition will be accepted within 30 days. Sorry, we can not accept returns of case studies, conference proceedings, sale items, or software (unless defective). Non-U.S. residents are responsible for payment of any taxes required by their government.